REPORT DOCUMENTATION PAGE

Form Approved
OMB No. 0704-0188

1. AGENCY USE ONLY (Leave blank)	2. REPORT DATE	3. REPORT TYPE AND DATES COVERED
	15 July 1997	Final Technical 3/1/95-2/28/97

4. TITLE AND SUBTITLE

Frequency Dependent Electrokinetic Studies of Rocks and Soils

5. FUNDING NUMBERS

F49620-95-1-0224

6. AUTHOR(S)

Frank Dale Morgan
Philip Reppert

AFOSR-TR-97

0342

7. PERFORMING ORGANIZATION NAME(S) AND ADDRESS(ES)

Earth Resources Laboratory
Dept. of Earth, Atmospheric, and Planetary Sciences
Massachusetts Institute of Technology
42 Carleton Street
Cambridge, MA 02142-1324

63118

9. SPONSORING/MONITORING AGENCY NAME(S) AND ADDRESS(ES)

AFOSR/NA
110 Duncan Avenue, Suite B115
Bolling AFB, DC 20332-0001

Contract Manager: Captain Michael Chipley

10. SPONSORING/MONITORING AGENCY REPORT NUMBER

11. SUPPLEMENTARY NOTES

12a. DISTRIBUTION/AVAILABILITY STATEMENT

Approved for Public Release; Distribution Unlimited

12b. DISTRIBUTION CODE

13. ABSTRACT *(Maximum 200 words)*

An experimental apparatus and data acquisition system was constructed to acquire frequency dependent streaming potential coupling coefficient information. The purpose of the experiments was to validate the frequency dependent theories of Pride and Packard. Frequency dependent streaming potential experiments were conducted on one glass capillary and two porous filters. Results indicated that both Packard's and Pride's models can fit the data. Experimentation continued on rocks. The new database and/or models can be used in seismoelectric models/interpretation and allow for the direct in situ determination of permeability. As a direct outcome of the research, a joint USAF/MIT patent disclosure was filed.

14. SUBJECT TERMS

Frequency dependent streaming potentials; seismoelectric effect; electrokinetic phenomena.

15. NUMBER OF PAGES

16. PRICE CODE

17. SECURITY CLASSIFICATION OF REPORT	18. SECURITY CLASSIFICATION OF THIS PAGE	19. SECURITY CLASSIFICATION OF ABSTRACT	20. LIMITATION OF ABSTRACT

TABLE OF CONTENTS

Executive Summary

Abstract

An experimental apparatus and data acquisition system was constructed to acquire frequency dependent streaming potential coupling coefficient information. The purpose of the experiments was to validate the frequency dependent theories of Pride and Packard. Frequency dependent streaming potential experiments were conducted on one glass capillary and two porous filters. The capillary has a diameter of 0.8 millimeters to 1.1 millimeters. The two porous filters have pore sizes that range from 70-100 and 145-175 micrometers. The results indicate that both Packard's and Pride's models can fit the data. Packard's model has one unknown model parameter while Pride's model has four unknown model parameters, two of which can be independently determined experimentally. Experimentation will now continue on rocks. The new data base and or models can then be used in seismoelectric models/interpretation and allow for the direct insitu determination of permeability. As a direct outcome of this research, a joint USAF/MIT patent disclosure has been filed. That aspect of this report should therefore be treated with appropriate confidentiality.

Objectives

The stated objectives of the proposal were to measure the frequency dependent electrokinetic properties of rocks and soils. *Specifically we were to measure the streaming potentials of rocks and soils from dc up through the seismic band (1000 Hertz).*

The preliminary stages of this research required that experimentation be conducted on capillary and porous filter samples with well characterized pore geometries. This initial step is required to establish a baseline for the performance of the experimental apparatus prior to using it on rocks and soils.

It was also an initial objective of this research to look at the effects of pore solution chemistry on the streaming potential frequency response of rocks and soils.

Summary of Results

The results presented in this report are the culmination of two years of research on a project originally intended as a three year project. Consequently, all of the objectives have not been as yet met. However, much progress towards completing all the objectives has been made.

An experimental apparatus has been constructed and tested, which allows testing of rocks and soils through 600 Hertz. Testing on glass capillaries and porous filters has verified the frequency dependent streaming potential theories of Packard and Pride. Now that experimental problems and calibrations have been worked out, testing of various rocks and soils will proceed expeditiously.

Experimentation was also conducted in the area of transient analysis of streaming potentials. This method shows some possibilities but may be limited by our present lack

of ability to create a fast enough transient to look at the frequency response of tight rocks. In some situations it may be preferable to work with the transient rather than the frequency behavior of in-situ rocks and soils.

Patents/Publications

Currently one patent proposal, *Electrodeless Streaming Potentials Measurements*, is being worked on as an outcome of this research project. Because this patent is still under development, it is asked that the AFSOR treat it with appropriate confidentiality. Brief information on it is contained in Appendix B, which has an attached patent disclosure form.

To date there have not been any publications or presentations of this research. Currently it is planned that a presentation will be made at the fall Annual Meeting of the American Geophysical Union. A detailed paper will also be published in the Journal of Geophysical Review.

Support

This research grant provided the main support to one Ph.D student, Philip Reppert, who is doing research in the area frequency dependent streaming potentials.

TECHNICAL REPORT

Introduction

The frequency dependent electrokinetic properties of rocks and soils are currently unknown, even though they are vital to our understanding of the electromagnetic signals generated by seismic waves propagating in the earth. It is believed that these electromagnetic signals are caused by fluid flow in rocks relative to the mineral matrix as a seismic wave passes through the rock. This relative flow induces a streaming current, which oscillates as an electric dipole at the same frequency as the seismic wave exciting the medium. The frequency dependent steaming current flows through the conductive rock to develop a frequency dependent streaming potential. Frequency dependent streaming potentials induced by a seismic wave will be referred to as the seismoelectric effect.

There have been numerous publications on steady state (DC) streaming potentials in the journals of Chemistry, Biology and Geophysics such as Morgan et. al. (1989), Ishido and Mizutani (1981), Kurtz et. al (1976), Levine et el. (1975), Rice and Whitehead (1965). However, despite the large volume of work in the area of DC streaming potentials very little work has been done in the area of frequency dependent streaming potentials. Past theoretical and experimental work dealing with the frequency response of streaming potentials was limited to three areas. One, to make frequency dependent streaming potential measurements at one frequency while varying the pressure in order to get plots of streaming potentials versus pressure without using a flow through apparatus (Sears & Groves, 1975). Two, to extrapolate the frequency dependent streaming potential value to

the DC limit for purposes of determining the zeta or mineral surface potentials. (Pengra et.al, 1995), (Wong, 1995), (Li et. al., 1995). Three, to examine the frequency dependent behavior of streaming potentials as a function of frequency, (Packard, 1953), (Cooke(1955). Packard (1953) proposed that the frequency dependent streaming potential coupling coefficient remains constant at its DC value until it approaches a critical frequency. Higher than the critical frequency, the streaming potential coupling coefficient decays with increasing frequency. Packard's experimentation was performed on a limited number of capillary samples of large radii and with no changes in solution chemistry. Packard was able to achieve a maximum measuring frequency of 200 Hz. Cooke (1955) attempted to duplicate Packard's work with limited success. Cooke reported that he could not match his capillary data to the theoretical curves of Packard. Cooke's shows for porous glass filters, Figure 1, appear to show the expected trend predicted by Packard's theory. (The data sets shown in Figure 1, are as Cooke lists them in his paper, no data set 1 is given.) However, on closer examination the curves do not appear to agree well with Packard's theory. Data set 2 has a fair fit for a capillary of diameter 127 micrometers but has only a few points in the transition region. Data set 3 appears to have a good fit to the theory for a capillary of diameter 155 micrometers but also has few points in the transition region. Data set 4 has only three points and conclusions cannot be drawn . Cooke does not provide information on pore geometries for the porous filters so further analysis of his results is purely speculative. *No one to date has satisfactorily fit frequency dependent streaming potential data to theoretical curves for porous media or for capillaries with diameters less than 155 micrometers.*

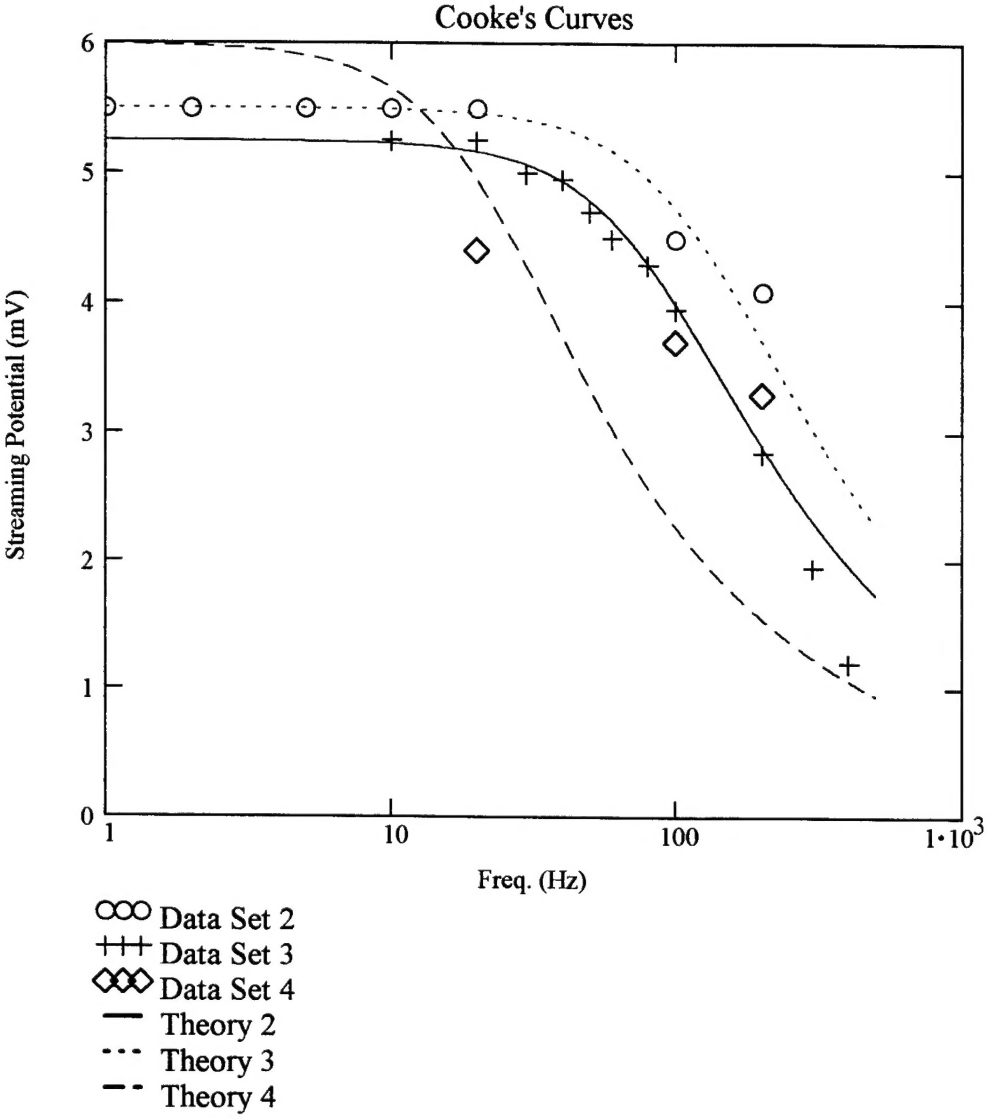

Figure 1- Comparison of Cooke's 1955 data with the best fit theorectical curves. Cooke did not provide dimensions for his samples. Estimated geometries based on data are given in this figure. Data set 2 has a fair fit to a capillary of 127 micrometers but has few points in the transition region. Data set 3 appears to have a good fit for a capillary of 155 micrometers, except at high frequencies. Data set 4 has only 3 points and conclusions cannot be drawn. (Adapted from Cooke, 1955)

Pride (1994) proposed a generalized theory for frequency dependent streaming potentials in porous media. No experimental work has been performed to validate the theory of Pride. Validation of Pride's theory is needed for a range of rock types and solution chemistries. The porous media theory of Pride can then be compared with the capillary theory of Packard. This in turn will provide valuable information, which can be used in the interpretation of seismoelectric signals. Other potential uses of this information range from the direct determination of insitu permeability to providing model parameters for electrical detection of earthquake precursors and underground explosions.

Since the seismoelectric effect was first observed by Ivanov (1939) there have been approximately twenty papers written on the subject. Within the past four years there has been a surge of eleven papers, both theoretical (Haartsen and Pride, 1994), (Haartsen, 1995), (Pride and Haartsen, 1996) and experimental (Thompson and Gist, 1993), (Mironov et. al, 1993), (Butler et. al, 1994), (Zhu et. al., 1994), (Haartsen et.al., 1995), (Kepic, 1995), (Wolf et. al., 1996) and (Mikhailov et. al., 1997). The seismoelectric experimental work has concentrated on detection and verification of the signals. This has been facilitated in the past five to ten years by advances in electronics and signal processing. The recent renewed interest in the seismoelectric effect only emphasizes the need for a thorough understanding of the appropriate physics and chemistry. *Full utilization of the seismoelectric effect cannot be achieved until the physics of the process are verified and model parameters are obtained for use during modeling and interpretation. No data beyond the critical frequencies exists for rocks.*

In order to adequately utilize the seismoelectric effect, the theory must be verified in the laboratory. This will entail performing tests on a variety of samples ranging from capillaries, and porous glass filters to real rocks. Each sample should be subjected to tests at a range of frequencies that go from well below the critical frequency to well above the critical frequency. All samples should be compared to the theories of Pride and Packard. Once the theory has been verified, testing should be conducted on a large database of real rocks to establish a data set for use in future seismoelectric interpretation.

Focus of This Research

In this research the results of Packard's theory will be compared to the results of Prides model. Once the theories have been developed, an explanation of the experimental setup will be provided. This will be followed by presentation of the data section where results for one glass capillary and two porous glass filters will be presented. These experiments will cover a frequency range of 1-500 Hz.

Theory

Streaming potentials are a subset of electrokinetic phenomenon, which includes electroosmosis, electrophoresis and sedimentation potentials. Electrokinetic phenomena are a consequence of a mobile space charge region that exists at the interfacial boundary of two different phases. The mobile space charge region occurs when two different phases are brought into contact with each other. This region is commonly referred to as the electrical double layer (EDL), it's most simplified approximations can be represented by a parallel plate capacitor (Helmholtz model) or a charge distribution that decays

exponentially away form the surface (Guoy-Chapman model). A more accurate model takes into account the finite size of ions by combining the Helmholtz and Guoy-Chapman models where a fixed layer exists at the surface (Stern layer) and a diffuse layer extends from the fixed layer into the bulk solution (Guoy-Chapman diffuse layer). This model is often referred to as the Stern model of the electrical double layer. More specifically the interfacial region consists of the inner Helmholtz plane (IHP) where ions are adsorbed to the surface and an outer Helmhotz plane (OHP) where ions are rigidly held by electrostatic forces and cannot move. The closest plane to the surface at which fluid motion can take place is called the slipping plane. The slipping plane has a potential defined as the zeta potential, which is characteristic of the solid and liquid that comprise the interface. The diffuse layer extends from the (OHP) into the bulk of the liquid phase. Figure 2 provides a schematic representation of the Stern model.

Streaming potentials occur when relative motion between the two phases displaces ions tangentially along the slipping plane by viscous effects in the water. This displacement of ions is referred to as convection current (I_{conv}) and has properties similar to an ideal current source. I_{conv} is given in equation (1) where ε is the dielectric

$$\mathbf{I_{conv}} = \frac{-\pi\varepsilon \mathbf{a}^2 \zeta \Delta \mathbf{P}}{\eta} \qquad \textbf{(1)}$$

constant, "a" is the radius of the capillary, ΔP is the pressure across the sample, η is the viscosity of the fluid and ζ is the zeta potential described earlier in the discussion on the electrical double layer. In steady state equilibrium the convection current must be

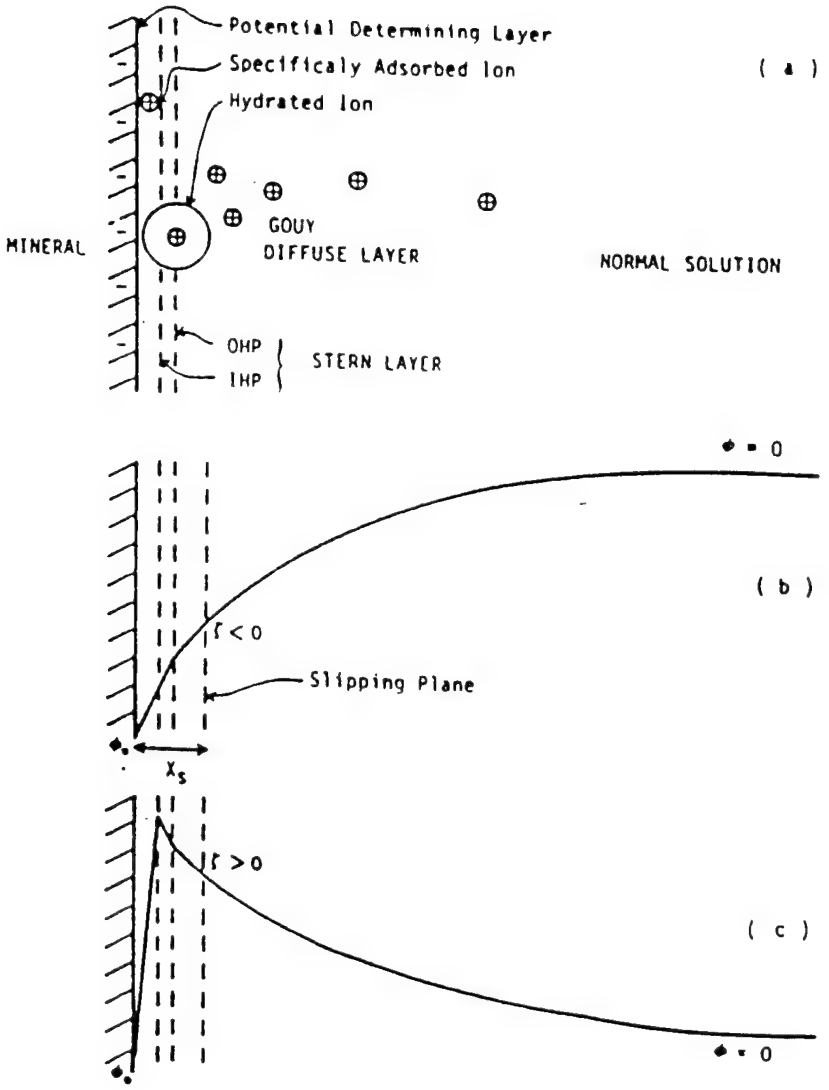

Figure 2 – (a) The Stern model of the electrical double layer. (b) The potential variation according to the Stern model (in the Stern layer the potential varies linearly). (c) The potential variation when the Stern layer contain more (positive) charge than is required to balance the (negative) charge on the solid. (Adapted from Ishido and Mitzutani, 1981)

balanced by a conduction current (I_{cond}), where σ is the fluid conductivity and ΔV is the voltage measured across the sample. Hence by ohms law,

$$\mathbf{I_{cond}} = \pi\sigma a^2 \Delta \mathbf{V} \qquad \textbf{(2)}$$

Figure 3 shows a schematic representation of fluid flow, convection current and conduction current.

Equating the convection and conduction currents, which must be equal at equilibrium, leads to the Helmholtz-Smoluchowski equation.

$$\Delta \mathbf{V} = -\frac{\varepsilon\zeta}{\eta\sigma}\Delta \mathbf{P} \qquad \textbf{(3)}$$

Details of the derivation of this classic expression can be found in texts such as, Colloid Science, (Kruyt, 1952). It should be noted when viewing this equation it is absent of geometry terms for the specimen. The ratio $\Delta V/\Delta P$ will be referred to as the cross coupling coefficient or simply the coupling coefficient for the remainder of the report. When the capillary or pore space dimensions approach the dimensions of the diffuse zone, (0.01 micrometer for 0.001 molar solution) surface effects must be considered. The samples to be used in this experiment do not approach these dimensions, hence these effects will not be addressed in this paper. However, the interested reader can obtain more information in Morgan et al. (1989) or Levine et al. (1975).

Now that the basic principles of steady state or DC streaming potential have been established, the principle of frequency dependent streaming potentials, also referred to as

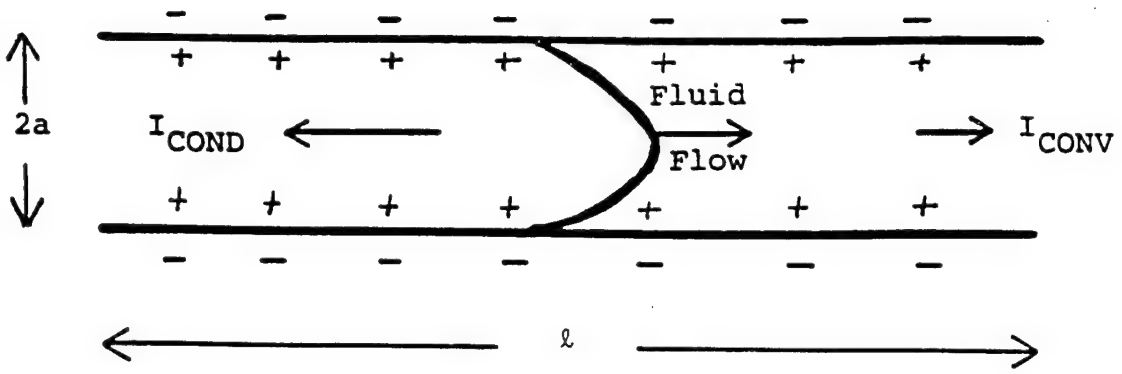

Figure 3 - Schematic diagram showing the relative flow of the fluid, convection current and conduction current.

dynamic streaming potentials or AC streaming potentials will be developed. The basic electrokinetic principles are the same in AC streaming potentials as in DC streaming potentials, however, instead of constant pressure applied across the sample the pressure is varied sinusoidally. As the frequency is increased, inertial effects in the fluid start to retard the motion of the fluid in the center of the pore space, as the fluid transitions from viscous dominated flow to inertial dominated flow. At higher frequencies the flow through the rock becomes inefficient. Therefore at frequencies higher than the transition from viscous to inertial flow it takes more pressure to shear the same quantity of ions from the diffuse zone than it does when strictly in the viscous flow regime. This can be seen in the equation (4), (Packard, 1953), for AC convection current in a capillary.

$$I_{convAC}(\omega) = \frac{-2\pi\varepsilon a\zeta}{\eta k}\frac{I_1(ka)}{I_0(ka)}Pe^{i\omega t} \qquad (4)$$

Where

$$k = \sqrt{-\frac{i\rho\omega}{\eta}} \qquad (5)$$

and ρ is the fluid density, ω is the angular frequency, I_0 and I_1 are Bessel functions.

Ohm's law for the AC conduction current equation is,

$$I_{condAC}(\omega) = V(\omega)\pi a^2\sigma / l \qquad (6)$$

Setting the AC convection and conduction currents equal at equilibrium leads to the AC Helmholtz-Smoluchowski equation

$$C_{AC}(\omega) = \frac{\Delta V(\omega)}{\Delta P(\omega)} = -\left[\frac{\varepsilon\zeta}{\sigma\eta}\right]\frac{2}{ka}\frac{I_1(ka)}{I_0(ka)} \tag{7}$$

The AC Helmhotz-Smoluchowski model reduces to the DC form, in the limit as ω goes to zero. Figure 4a shows the AC coupling coefficient and Figure 4b shows the associated phase response for several capillary sizes. The critical frequency, where the flow transitions from viscous dominated flow to inertial dominated flow, is given by,

$$\omega_c = \frac{a^2\eta}{8\rho} \tag{8}$$

In 1994, Pride presented a generalized model for AC streaming potentials in a porous media. Pride's version of the AC Helmholtz-Smoluchowski equation is given in by,

$$CP_{AC} = \frac{\Delta V(\omega)}{\Delta P(\omega)} = \left[\frac{\varepsilon\zeta}{\eta\sigma}\right]\left[1 - i\frac{\omega}{\omega_t}\frac{m}{4}\left(1 - 2\frac{d}{\Lambda}\right)^2\left(1 - i^{\frac{3}{2}}d\sqrt{\frac{\omega\rho}{\eta}}\right)^2\right]^{-\frac{1}{2}} \tag{9}$$

where CP_{AC} represents the AC coupling coefficient for porous media, the Debye length is given by d, and Λ is typical pore radius, representing a weighted volume-to-surface ratio, (Pride, 1994). The dimensionless number *m* is defined as

$$m \equiv \frac{\phi}{\alpha_\infty k_0}\Lambda^2 \tag{10}$$

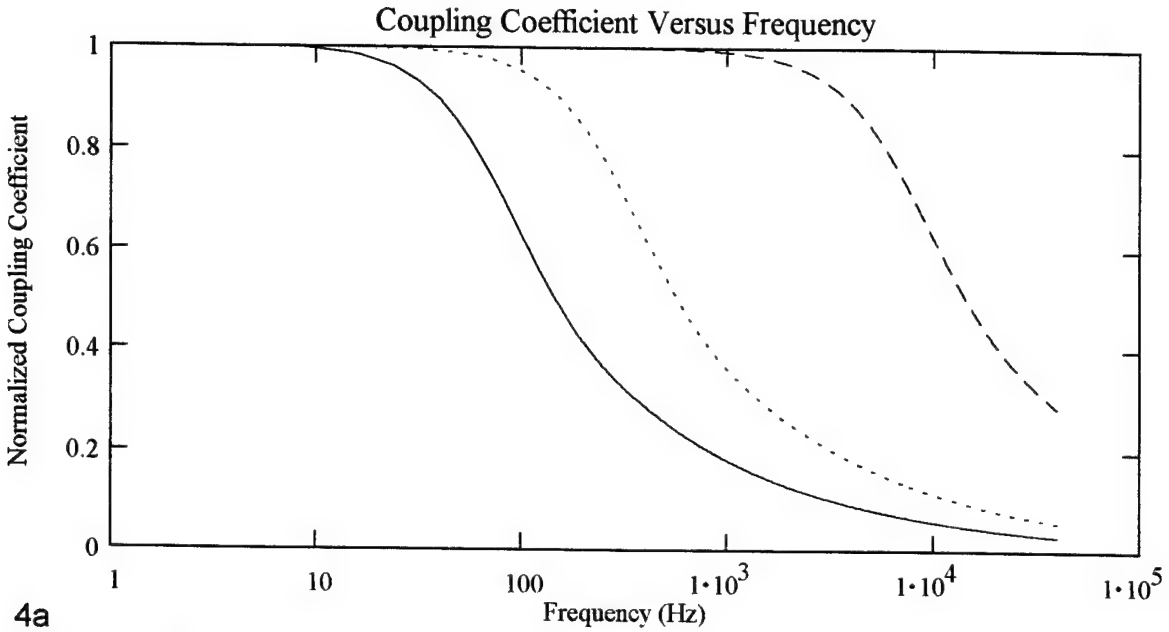

4a

— Pore Radius is 100 microns
- - - Pore Radius is 50 microns
– – Pore Radius is 10 microns

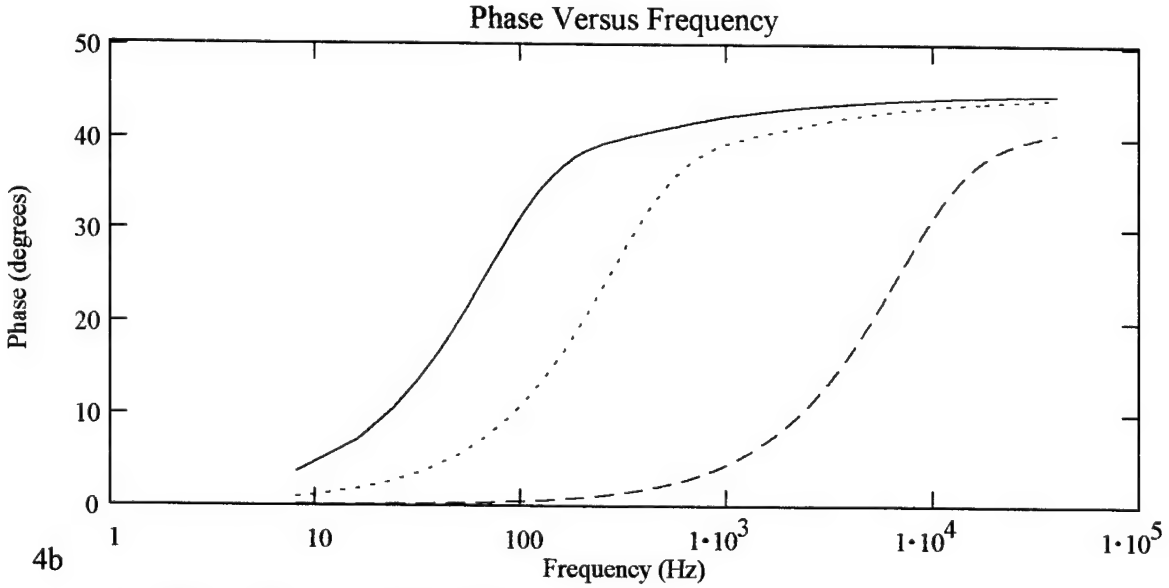

4b

— Pore Radius is 100 microns
- - - Pore Radius is 50 microns
– – Pore Radius is 10 microns

Figure 4a & 4b - Figure 4a shows the normalized coupling coefficient for three capillaries of differentradii. Figure 4b shows the phase associated with the coupling coefficient for the same three capillaries.

and consist of pore-space geometry terms. It reduces to 8 for a capillary and in fact usually has the same value for porous media and rocks. Correspondingly the generalized equation for the critical frequency, ω_t, for porous media is given in by,

$$\omega_t \equiv \frac{\phi}{\alpha_\infty k_0}\frac{\eta}{\rho} \qquad (11)$$

where porosity is given by ϕ, tortuosity is given by α_∞ and the DC permeability is k_0.

Examination of the AC porous media coupling coefficient indicates that to first order the response is determined by the critical frequency ω_t and the DC coupling coefficient. When capillary geometry terms are used in the Pride's AC porous media coupling coefficient, equation (9), the results reduce to results that are similar but not identical but virtually indistinguishable to those generated using the Packard's AC capillary coupling coefficient, equation (7). The comparison of Packard's and Pride's models can be seen in Figure 5. The slight discrepancy between the two curves is due to the analytical expression developed by Pride which combines the low frequency and high frequency equation for the coupling coefficient.

Experimental Approach

The approach used to verify the theory, was to hold the capillary or porous filter stationary and oscillate the fluid back and forth through the sample using a sinusoidal driving pressure at one end while having the other end open to the atmosphere. Silver-silver chloride electrodes are placed on either side of the sample in fluid dead legs to keep them out of possible fluid flow paths, (Morgan et al., 1989). The frequency response of

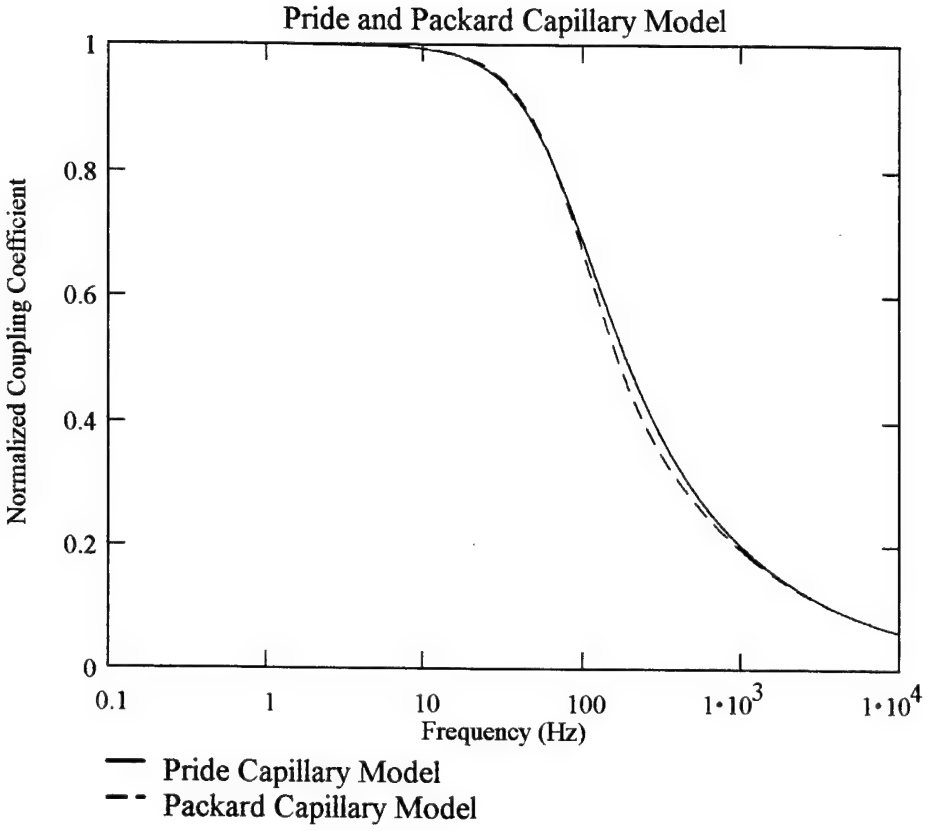

Figure 5 - Comparison of Packard's and Pride's model for a capillary

the electrodes was measured and found flat in the region used in this testing. The electrode measurements were also verified through use of a capacitive coupled antenna placed around the outside of the sample. The pressure was monitored on the high-pressure and low-pressure sides of the sample by miniature hydrophones that have a flat frequency response from 1-20000 Hz. The apparatus, which holds the sample, electrodes and hydrophones is constructed of plexiglass and is schematically shown in Figure 6. A photograph of the test cell is shown in Figure 7. The enclosure around the sample and preamplifiers is constructed of Mu-metal. The plexiglass housing which holds the sample is additionally enclosed in an aluminum housing. The electromechanical shaker is enclosed in a steel box. The large amount of shielding is required for two reasons. The first is due to the fact that the laboratory is an electrically noisy environment. The second reason is that the pressure is being driven by an electromechanical transducer, which is driven at the same frequency as the one being measured in the apparatus. The driving transducer and associated leads emit enough EMF, at the same frequency to affect the measured results. Depending on the pore or capillary diameters, the resistance of the sample could be several hundred megaohms, which acts as an antenna for the EMF fields of the electromechanical transducer. The entire plexiglass housing was weighted down with 100 pounds to reduce any sample vibration.

Data collection was achieved using two instrument preamplifiers and a 12-bit analog-to-digital board with 24.8 microvolt resolution. The electrometer preamplifiers were required as input buffers due to the potentially high impedance of the samples (.5 MΩ to

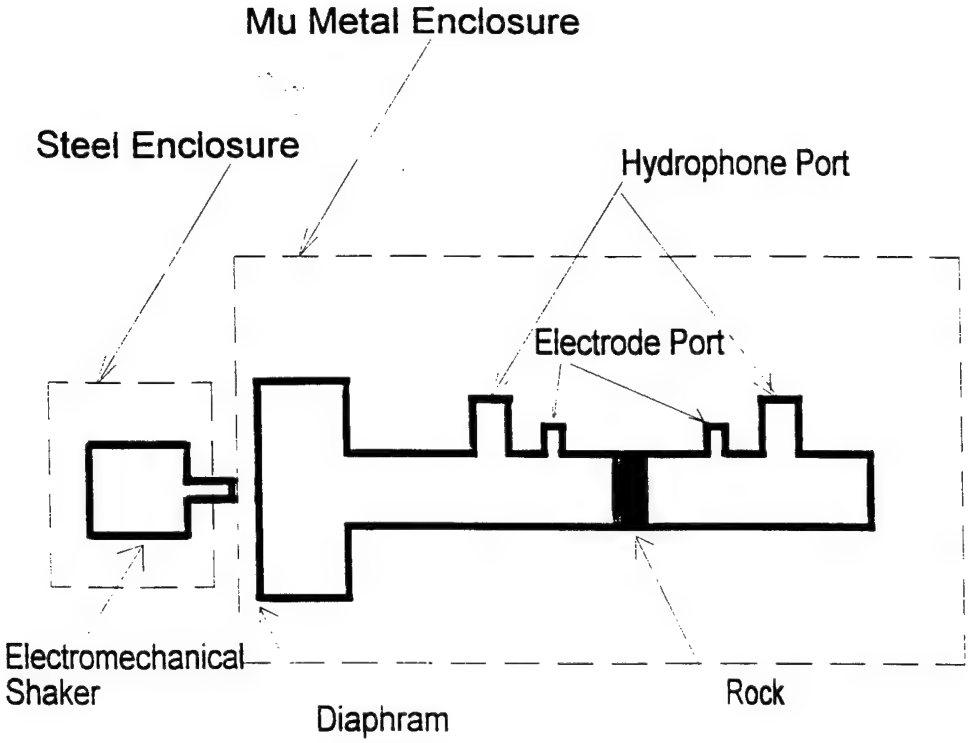

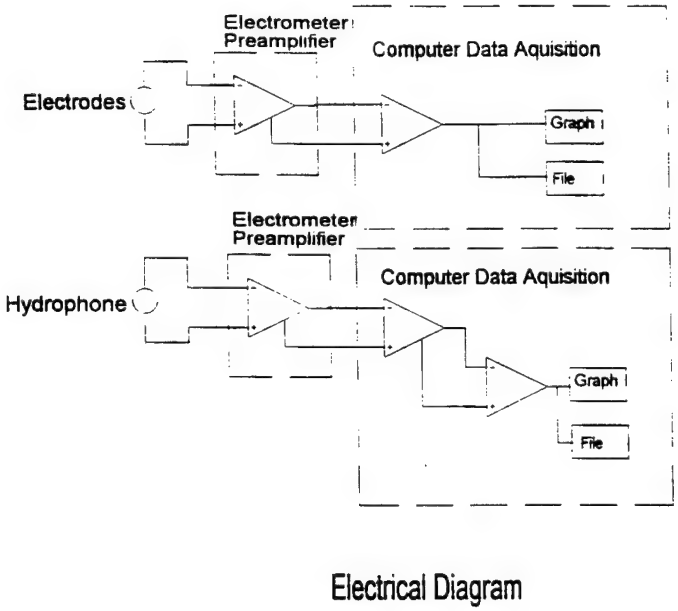

Figure 6 - Schematic representation of the mechanical and electrical layout of the experimental setup.

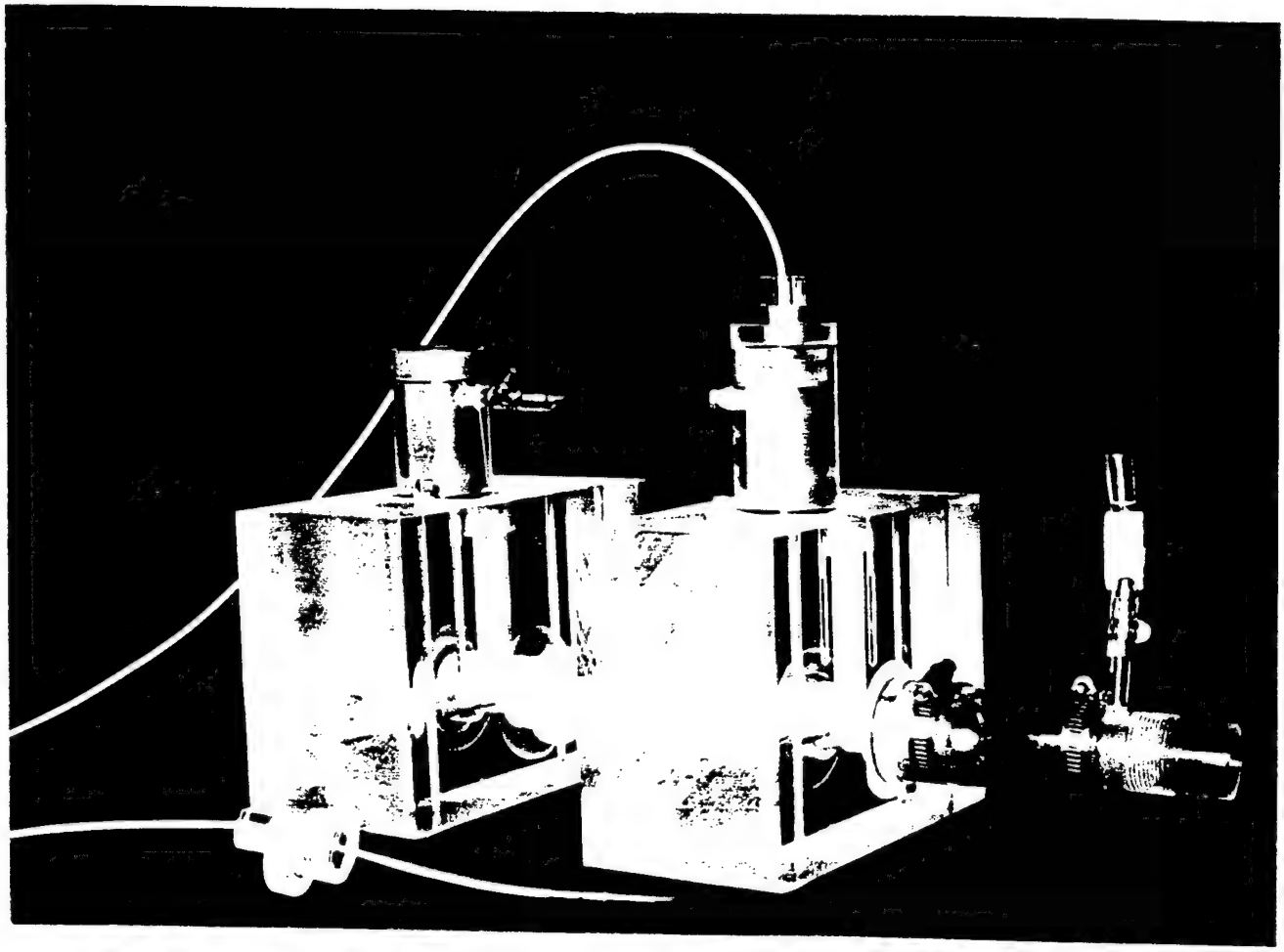

Figure 7 - Photograph of the experiment test cell used for testing of frequency dependent streaming potentials

300 MΩ). For a schematic representation of the data acquisition system please refer to Figure 6. The amplitude spectram of the time domain signals, voltage and pressure were taken and the amplitude ratios were measured at the driving frequency. The raw data was saved for possible future processing.

Data/Results

Specimens

The capillary, (capillary 1), has an inner diameter that can range from 1.1 mm to 0.8 mm. The length of capillary 1 is 60 centimeters. The first porous filter, (porous filter A), has pore sizes ranging from 145 to175 μm. Porous filter A has a diameter of 1 centimeter and a thickness of 2 millimeters. The second porous filter, (porous filter B), has pore sizes ranging from 70 to100 μm. Porous filter B has a diameter of 2 centimeters and a thickness of 2 millimeters.

Figure 8a, shows data of the coupling coefficient versus frequency for capillary 1. Each data point is the mean of 6 measurements with the standard deviation shown. The best fit Packard theoretical curve is plotted through the data points. The curve fits the data points within experimental accuracy and provides good correlation at lower to middle frequencies. At the higher frequencies the standard deviation remains small even though the data starts to diverge slightly from the curve. The last data point has a large standard deviation and is the result of a poor signal to noise ratio. The measured critical frequency for capillary 1 is 7.1 Hz and the calculated critical frequency from the manufacture's capillary dimensions is 3-7.1 Hz. Figure 8b shows the coupling coefficient phase versus

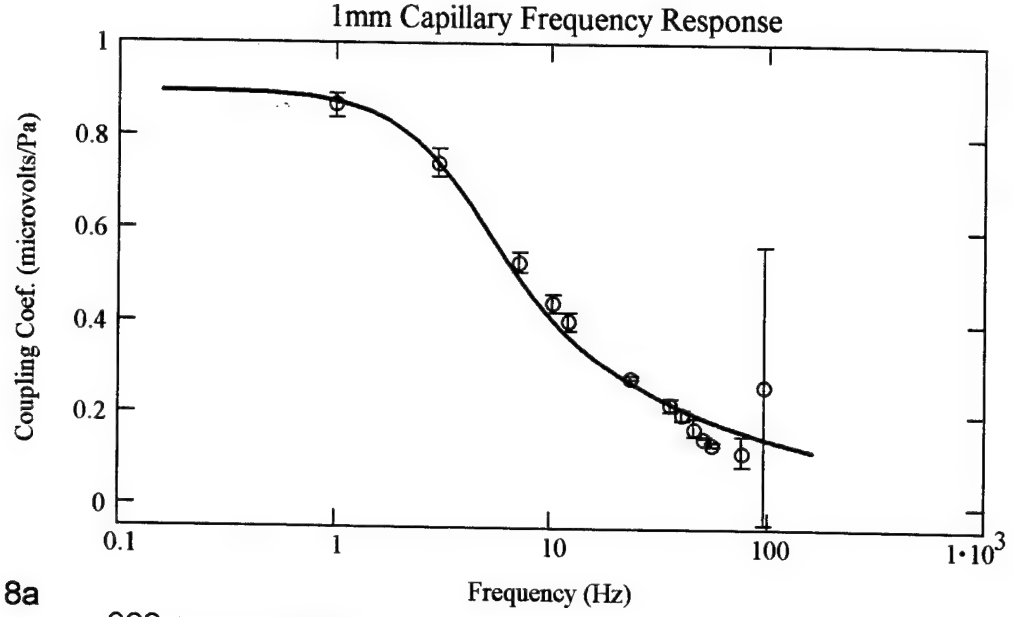

8a

ooo 1 mm Capillary
I 1 mm capillary error bar
— Theory

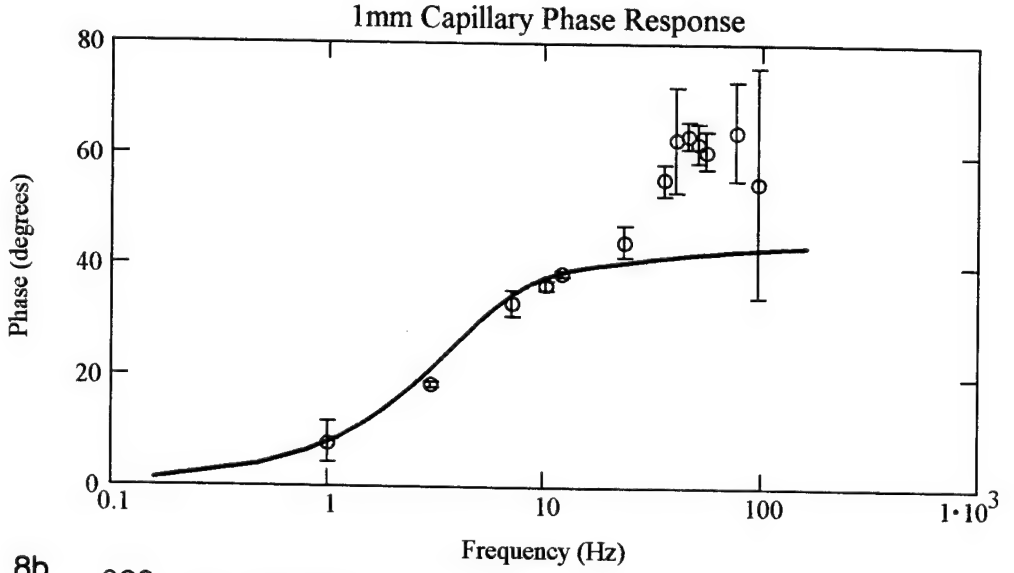

8b

ooo 1 mm capillary
I 1 mm capillary error bar
1 m capillary error bar
— Theory

Figure 8a & 8b - Figure 8a shows cross coupling frequency response data with error bars for a 1mm capillary plotted along with the theory for a 1mm capillary. Figure 8b shows the cross coupling phase response for a 1 mm capillary along with the theory.

frequency for capillary 1. The phase measurements appear to be in fair agreement with the theory curves also plotted in figure 8b. The phase data tracks the theory curve until the coupling coefficient starts to diverge from the theory. Then the phase goes to approximately 65 degrees and remains constant.

The porous filter A data is plotted against Pride's and Packard's theories in Figure 9. As can be seen in Figure 9 both models fit the data well, although Packard's model may be a slightly better fit for the last three data points. This difference between Parkard's and Pride's models was discussed earlier and determined to be due to the merging of the Pride's low and high frequency analytical expressions into a single analytical equation. For porous filter A, both Packard's and Pride's models give a critical radius of 175 micrometers. The manufacture provided pore size for the porous A filter is 145-174 micrometers.

Figure 10a shows the frequency response for both porous filter A and porous filter B. The dimensions of porous filter A were determined above to be 175 micrometers. Porous filter B has its best fit to the theoretical curve for a 110 micrometer pore diameter. Recall that the pore radius given by the manufacturer is 70 to 100 micrometers. The data for porous filter B fits the data well in the low frequency and high frequency region but diverges from the theory in the transition region. This divergence of the data may be an artifact of minimal data averaging for this sample. Phase curves for porous filter A are shown in Figure 10b. As can be seen in this figure the measured phase is in good agreement with the theoretical curves.

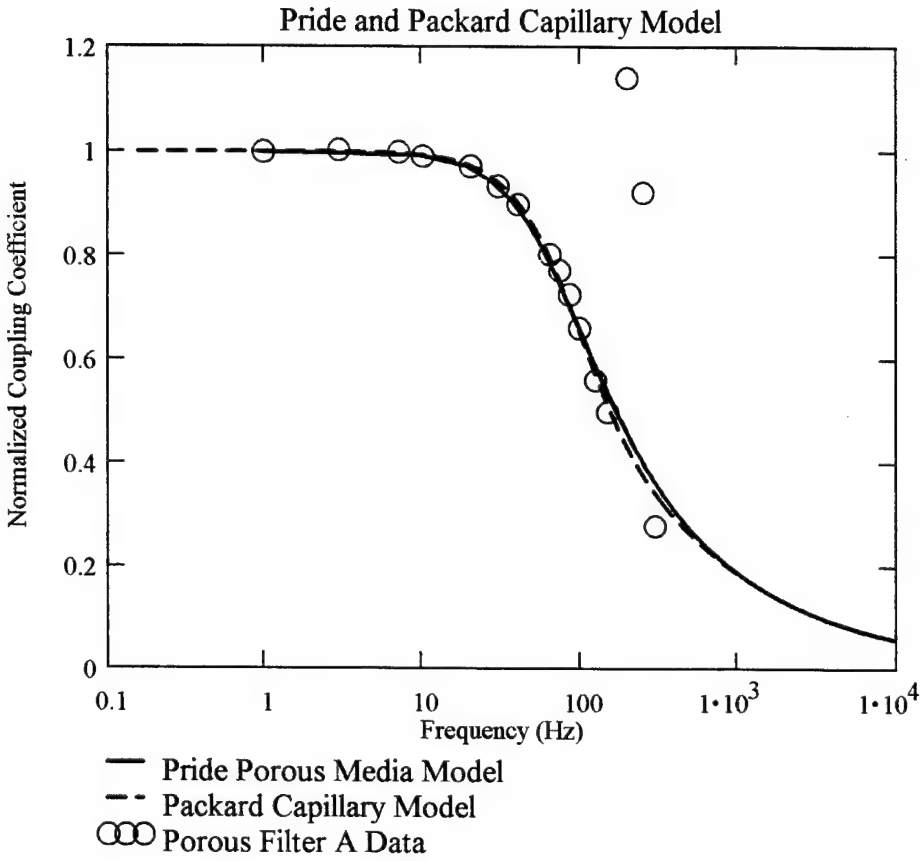

Figure 9 - Comparison of Packard's and Pride's model to the data for porous filter A. Packard's model gives a pore radius of 175 micrometers. Pride's model gives a radius of 175 micrometer when using a formation factor of 3. The maufacture gives the pore dimensions as ranging from 145-175 micrometers.

10a

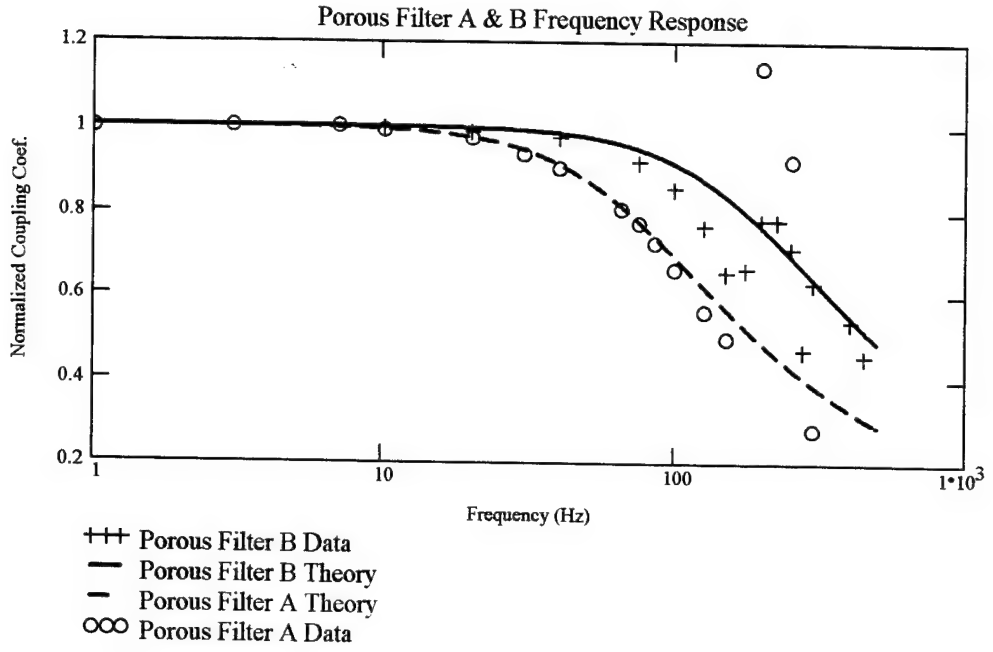

10b

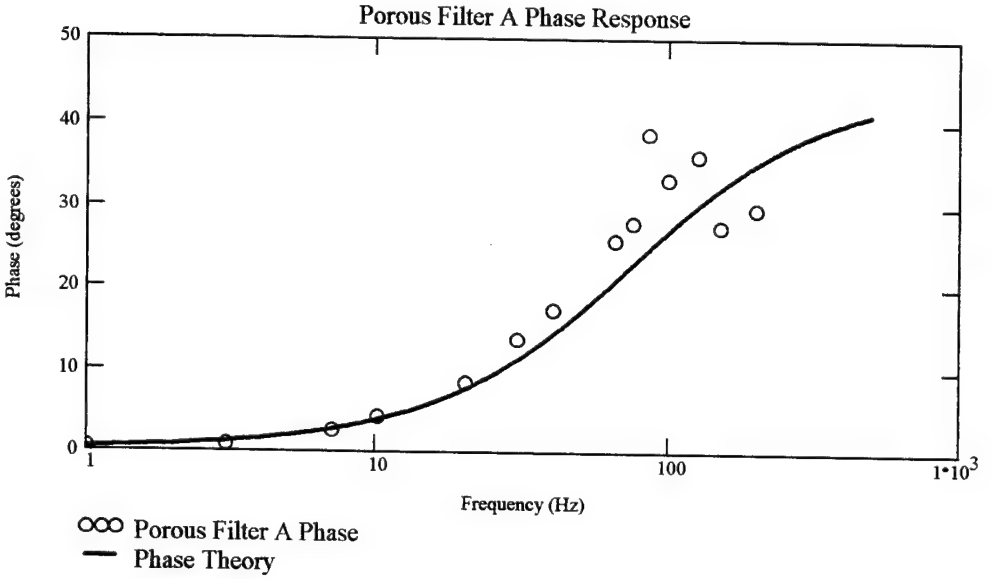

Figure 10a & 10b - Figure 10a shows cross coupling frequency response data for porous filter B plotted along with the theory for a 110 micrometer porous filter. Figure 10a also shows the response for porous filter A along with the theory for a 175 micrometer porous filter. Figure 10b shows the cross coupling phase response for porous filter A.

Discussion and Applications

The emphasis of this study has been the verification of Packard's and Pride's theory over a range of pore sizes. Both theories fit the data identically when using m = 8 in Pride's equation. It has been observed that most rocks have 8 as the value for m, therefore this approximation is reasonable. The important parameter to determine from frequency dependent streaming potential curves is the critical frequency. The critical frequency can be determined graphically from the data or by curve fitting the theory to the data and then determining the critical frequency from the theory. In Packard's theory for a capillary the critical frequency is related to the radius, viscosity and density of the fluid. In Pride's model one additional parameter, m, is included, if the second order parameters are neglected. These second order parameters are important where the pore sizes are small and/or the electrolyte concentration is low.

It can therefore be inferred from the data on glass filters that for rocks with pore diameters much larger than the diffuse zone, the theories of Pride and Packard cannot be distinguished from each other. What is different is the way in which the critical frequency is related to the governing physical and chemical parameters. In this respect, Pride's model is more complete and general.

Experimentation has shown that external vibration entering the system can skew the results. In fact preliminary experiments indicate when the matrix is excited without driving the fluid, the coupling coefficient is much higher than when the fluid is excited

and the matrix is held stationary. Consequently, care must be exercised while exciting the fluid and holding the matrix stationary. This will be the focus of future research, to fully understand this phenomenon.

Electroseismic Interpretation

A large data base of coupling coefficients will be useful in seismoelectric interpretation because the frequency dependent amplitude of the seismoelectric response will in large part be due to the coupling coefficient of the rock fluid interface.

Use of the critical frequency in the seismoelectric effect, to predict permeability, appears to be limited to very porous materials or the detection of fractures in intact rock. Seismoelectric experiments are limited to seismic frequencies (DC-1000 Hz), which limits the use of critical frequencies to permeabilities ranging from 0.1 Darcy to 10 Darcies. This can be seen in Figure 11, which shows how permeability is related to the critical frequency.

There is some concern of being able to fully utilize streaming potentials in the seismoelectric field. This arises from the questions raised about the potential non-reciprocity of the fluid moving relative to the matrix and the matrix moving relative to the fluid. So far all theory has treated this as a reciprocal problem and no detailed examination of the effect of moving the solid relative to the fluid has been addressed.

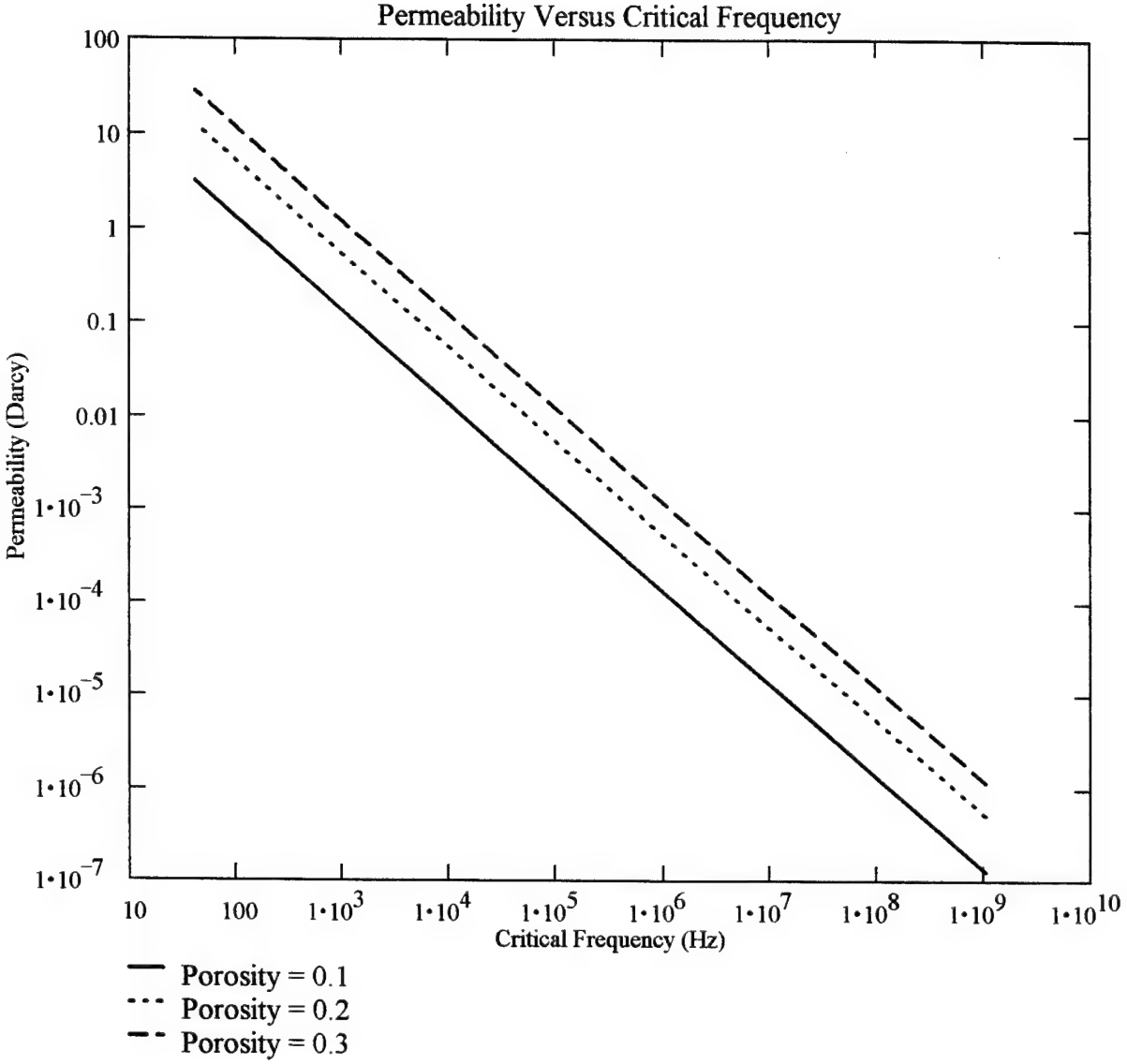

Figure 11 - Permeability versus critical frequency for rocks with porosities of 0.1, 0.2, and 0.3.

Permeability

Use of frequency dependent streaming potentials appears to have good potential for use in the determination of permeability in the laboratory and possibly under field conditions. There are two different modes that can be used for the determination of permeability, the critical frequency method and pressure versus streaming potentials method.

The critical frequency method of determining permeability is based on determining the critical frequency and formation factor of the rock, along with the viscosity and density of the pore fluid. Equation 10, shown again below in another form, with $\alpha=F\phi$ can be used to determine the permeability of the rock.

$$k_o = \frac{1}{F\omega_t}\frac{\eta}{\rho} \qquad \textbf{(14)}$$

This method of determining permeability appears to be limited to frequencies below 20 kHz - 30 kHz, which corresponds to permeabilites greater than 4 millidarcy, see Figure 11. This limitation in the laboratory, is due to pressure source limitations and considerations concerning standing waves in the system. Laboratory limitations must be fully understood before attempting to apply this method in the field.

Future Work

Many different research directions can be taken as a continuation of this study. The major directions that can be undertaken in the near future are,

- Extend the frequency range of the present experiment to 20 kHz - 30 kHz.

- Understand and model the process that is occurring when the source of the vibration is through the solid matrix..
- Perform frequency dependent studies at insitu temperature and pressure to better ascertain what is happening to the solution chemistry as well as the electrical double layer.

Summary/Conclusion

A comparison of streaming potential data to proposed models has been presented for various pore sizes. Although there is a slight discrepancy between the capillary model and the generalized model, as a whole both Packard's and Pride's models are able to predict the capillary data. However, the data tends to fit the Packard's model better in the region of divergence between the models. For Porous media both Pride's porous media model and Packard's capillary model predict accurately the form the data should take. The difference between the two models shows up in the model parameters used to fit the curve.

Acknowledgements

We wish to thank David Lesmes, Laurence Jouniaux for their assistance and guidance in helping to get this project started. We would also like to thank Derick Hirst and the Laboratory of Nuclear Science Machine Shop personnel for their invaluable help in constructing the test cell and other required equipment.

References

1. Butler, K. E., Russell, R. D., Kepic, A. W., and Maxwell, M., Mapping of a Stratigraphic Boundary by it's Seismoelectric response: Proc. 1994 SAGEEP Ann. Mtg., 689-699, 1994.

2. Cooke, C.E., Study of Electrokinetic Effects Using Sinusoidal Pressure and Voltage, Journal of Chemical. Physics, 1955, 23, 2299.

3. Haartsen, M. W., Coupled Electromagnetic and Acoustic Wavefield Modeling in Poro-Elastic Media and its Application in Geophysical Exploration: Ph.D. thesis, Mass. Inst. of Tech, 1995.

4. Haartsen, M.W., and Pride, S. R.., Modeling of Coupled Electroseismic Wave Propagation from Point Sources in Layered Media: 64the Ann. Intenat. Mtg.c Soc. Expl. Geophys., Expanded Abstracts, 1994, 1155-1158.

5. Haartsen, M. W., Zhu, Z., and Toksoz, M. N., Electroseismic Method for Mapping the Oil-Water Interfaces: Presented at the Dharam, Saudi Arabia, Soc. Petr. Eng., 1995.

6. Ishido, T., and Miztani, H., Experimental and Theoretical Basis of Electrokinetic Phenomona in Rock-Water, J. Geophysical Review, 86, 1763-1775, 1981.

7. Ivanov, A. G., Effects of Electrization of Earth Layers by Elastic Waves Passing Through Them (in Russian): Doklady Akademii Nauk SSSR, 24, No. 1, 41-43.

8. Kepic, A.W., Maxwell, M., and Russel, R. D., Field Trials of Seismoelectric Method for Detecting Massive Sulfides, Geophysics, 60, Number 2, 365-373, 1995.

9. Kruyt, H. R., Colloid Science, Volume 1. Irreversible Systems, Elsevier Publishing Company, New York, 1952.

10. Kurtz, R. J., Findl, E., Kurtz, A. B., and Stormo, L. C., Turbulent Flow Streaming Potentials in Large Bore Tubing, J. Colloid Interface Sci., 57, 28-39, 1976.

11. Levine, S., Marriott, J. R., Neale, C., and Epstein, N., Theory of Electrokinetic Flow in Fine Cylindrical Capillaries at High Zeta Potentials., J. Colloid Interface Sci., 52, 136-149, 1975.

12. Li, S. X., Pengra, D. B., and Wong, P., Onsager's Recipocal Relation and the Hydraulic Permeability of Porous Media, Physical Rev. E, 51, Number 6, 5748-5751, 1995.

13. Mikhailov, O.V., M.W. Haartsen and M.N. Tokoz, Electroseismic Investigation of the Shallow Subsurface: Field Measurements and Numerical Modeling, Geophysics, 1997, Volume 62, Number 1, 1-9.

14. Mironov, S. A., Parkhomenko, E. I., and Charnyak, G. Y., Seismoelectric Effects of Rocks Saturated with Gas or Liquid Hydrocarbons, Izv. Acad. Sci. USSR, Physics of the Solid Earth, 1993.

15. Morgan, F.D., E.R. Williams, and T.R. Madden, Streaming Potential Properties of Westerly Granite with Applications, J. Geophys. Res., 94, 12449-12461, 1989.

16. Packard, R. G., Streaming Potentials Across Glass Capillaries for Sinusoidal Pressure, Journal of Chemical Physics, 1953, 21, 303.

17. Pengra, D.B., P. Wong, Electrokinetic Phenomena in Porous Media, Disordered Materials and Interfaces - Fractals, Structure and Dynamics, MRS Conference Proceedings, Boston, December 1995.

18. Pride, S., Governing Equations for the Coupled Electromagnetics and Acoustics of Porous Media, Physical Review B, 1994, Volume 50, Number 21, 15678-15696, 1994.

19. Pride, S. R., Haartsen, M. W., Electroseismic Wave Properties, J. Acoust. Soc. Am., 100, 1301-1315, 1996

20. Rice, C. L., and Whitehead, R., Electrokinetic Flow in a Narrow Cylindrical Capillaries, Journal of Physical Chemistry, 69, Number 11, 1965.

21. Sears, A.R., and J.N. Groves, The Use of Oscillating Laminar Flow Streaming Potential Measurements to Determine the Zeta Potential of a Capillary Surface, Journal of Colloid International Science, 1977, 65, 479.

22. Thompson, A. H. and G.A. Gist, Geophysical Application of Electrokinetic Conversion, The Leading Edge, December 1993, 1169.

23. Wong, P., Determination of Permeability of Porous Media by Streaming Potential and Electro-osmotic Coefficients, US Patent, Patent Number 5,417,104, 1995.

24. Wolfe, P.J., Yu, J., and Gershnzon, N., Seismolectric Studies in an Outwash Plain, Proc. 1993 SAGEEP Ann. Mtg., 21-30, 1996

25. Zhu,Z., Cheng, C., Toksoz, M. N., Electroseismic Conversion in a Fluid Saturated Porous Rock Sample, 64th Ann. Internat. Mtg. Soc. Expl. Geophys., Expanded Abstracts, 26-29, 1994.

Appendix A

The capacitive coupled antenna, consist of a piece of copper tubing that is placed around the outside of the sample. The copper tubing is then connected to the positive input of the instrument amplifier. The negative input to the instrument amplifier is connected to ground. The copper tubing detects the electric field being emitted by the sample. The measured streaming potential frequency response must then be corrected for the gain of the antenna. Figure A1 show data collected on capillary one sample, while using the antenna. As can be seen in this figure, the antenna results have good correlation to the theory.

As part of this patent, we are also examining the use of an inductively coupled antenna to use in directly monitoring streaming current.

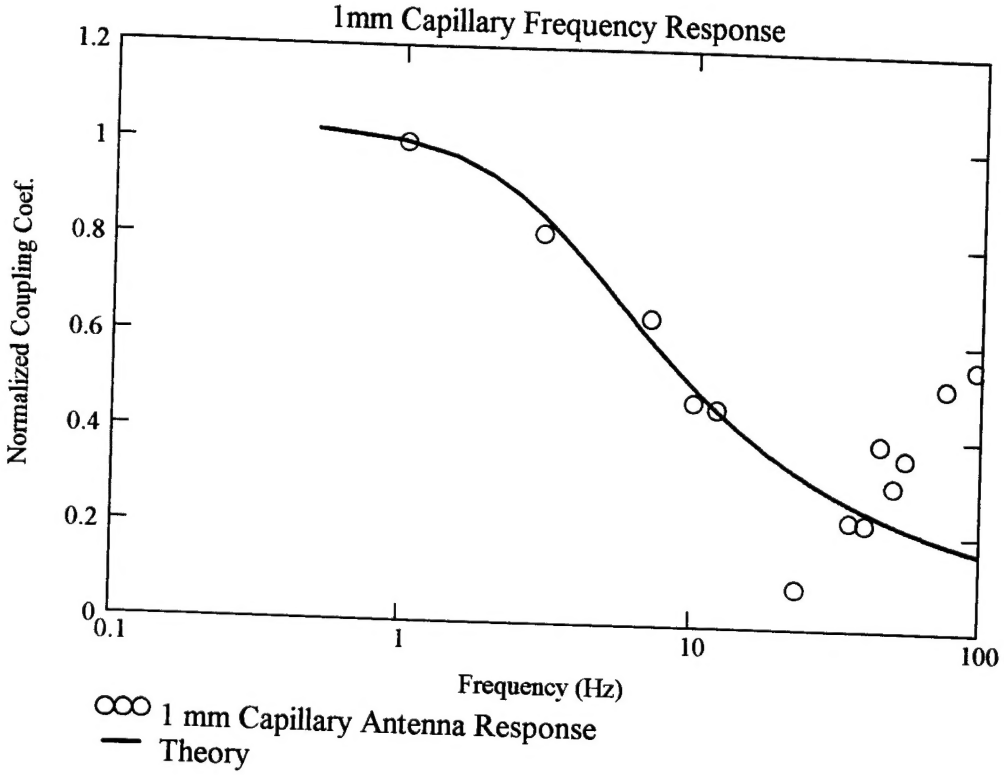

Figure A1 - 1 mm capillary coupling coefficient frequency response using an antenna instead of electrodes.